Inorg. Chem. **2007**, *46*, 4592–4598

Inorganic Chemistry
Article

Transformation of $AeIn_4$ Indides (Ae = Ba, Sr) into an $AeAu_2In_2$ Structure Type Through Gold Substitution

Jing-Cao Dai[†] and John D. Corbett*[,‡]

Ames Laboratory, DOE and Department of Chemistry, Iowa State University, Ames, Iowa 50010, and Institute of Materials Physical Chemistry, Huaqiao University, Quanzhou, Fujian 362021, China

Received January 26, 2007

The title compounds were prepared from the elements by high-temperature solid-state synthesis techniques. X-ray structural analyses shows that $BaAu_2In_2$ (**1**) and $SrAu_2In_2$ (**2**) crystallize in a new orthorhombic structure, *Pnma*, $Z = 4$ ($a = 8.755(2)$, 8.530(2) Å; $b = 4.712(1)$, 4.598(1) Å; $c = 12.368(3)$, 12.283(4) Å, respectively). Gold substitutes for 50% of the indium atoms in the tetragonal $BaIn_4$ and monoclinic $SrIn_4$ parents to give this new and more flexible orthorhombic structure. The Ae atoms in this structure are contained within chains of hexagonal prisms built of alternating In and Au that have additional augmenting atoms around their waists from further condensation of parallel displaced chains. The driving forces for these structural changes are in part the shorter Au–In distances (2.72 and 2.69 Å) relative to *d*(In–In) in the parents, presumably because of relativistic contractions with Au. Generalities about such centered prismatic building blocks and their condensation modes in these and related phases are described. Band structure calculations (EHTB) demonstrate that the two compounds are metallic, which is confirmed by measurements of the resistivity of **1** and the magnetic susceptibilities of both.

Introduction

Explorations of polar intermetallic phases formed between the triel elements (Tr = Al−Tl) and the electropositive alkali (A) or alkaline-earth (Ae) metals have led to discovery of a variety of remarkable features about their chemistries: unanticipated stoichiometries, fascinating structures, and evidently novel bonding features. Substantial deviations from classical valence viewpoints and Zintl concepts are found among the structures of and bonding in even the binary compounds between the active metals and the early p-elements, challenging our general understanding.[1−3] The electronic structures of these polar intermetallic phases are often remarkable; some have excess electronic counts relative to classical valence rules, as in K_8Tr_{11}[4] and $K_{10}Tl_7$,[5] and others are clearly electron deficient, as with $Na_4K_6Tl_{13}$,[6] $K_8In_{10}Zn$,[7] and $Na_2K_{21}Tl_{19}$.[8] The complexity of the structures, especially the degree of condensation among the more electronegative elements, increases with higher-charged cations or a lower proportion of the active metal component, as in $SrIn_4$[9] and $K_{39}In_{80}$.[10] Moreover, the addition of electron-poorer late transition (d) elements to these triel systems further removes the products from classical electron-counting regimes and closed-shell notions and into the less understood general area of polar intermetallics. The use of gold in the last role has been found to be additionally attractive because of the usual lattice and bond length contractions this element brings about through relativistic effects, that is, in Ba_2AuTl_7,[11] $BaAuIn_3$, and $BaAuTl_3$,[12] $BaAu_xIn_{2-x}$,[13] $Ca_2Au_3In_4$,[14]

* To whom correspondence should be addressed. Email: jdc@ameslab.gov.
‡ Iowa State University.
† Huaqiao University.

(1) (a) Nesper, R. *Angew. Chem., Int. Ed. Engl.* **1991**, *30*, 789. (b) Belin, C. H. E.; Tillard-Charbonnel, M. *Prog. Solid State Chem.* **1993**, *22*, 5.
(2) (a) Corbett, J. D. In *Chemistry, Structure and Bonding of Zintl Phases and Ions*; Kauzlarich, S. M., Ed.; VCH Publishers: New York, 1996; Chapter 4. (b) Corbett, J. D. *Angew. Chem., Int. Ed.* **2000**, *39*, 670.
(3) Miller, G. J.; Lee, C.-S.; Choe, W. In *Inorganic Chemistry Highlights*; Meyer, G., Naumann, D., Wesemann, L., Eds.; Wiley-VCH Verlag-Gmbh: Weinheim, Germany, 2002; Chapter 2.
(4) Sevov, S. C.; Corbett, J. D. *Inorg. Chem.* **1991,** *30*, 4875.
(5) Kaskel, S.; Corbett, J. D. *Inorg. Chem.* **2000**, *39*, 3086.
(6) Dong, Z.-C.; Corbett, J. D. *J. Am. Chem. Soc.* **1995**, *117*, 6447.
(7) Sevov, S. C.; Corbett, J. D. *Inorg. Chem.* **1993**, *32*, 1059.
(8) Dong, Z.-C.; Corbett, J. D. *J. Am. Chem. Soc.* **1994**, *116*, 3429.
(9) Seo, D.-K.; Corbett, J. D. *J. Am. Chem. Soc.* **2000**, *122*, 9621.
(10) Li, B.; Corbett, J. D. *Inorg. Chem.* **2003**, *42*, 8768.
(11) Liu, S.; Corbett, J. D. *Inorg. Chem.* **2004**, *43*, 2471.
(12) Liu, S.; Corbett, J. D. *Inorg. Chem.* **2004**, *43*, 4988.
(13) Dai, J.-C.; Corbett, J. D. *Inorg. Chem.* **2006**, *45*, 2104.
(14) Hoffmann, D.-R.; Poettgen, R. *Z. Anorg. Allg. Chem.* **1999**, *625*, 994.

10.1021/ic070142v CCC: $37.00
Published on Web 04/17/2007

$Ce_2Au_3In_5$,[15] and KAu_4In_2.[16] There is another factor in the stability of such polar intermetallic phases, beyond the general importance of size and high coordination numbers: the additional Madelung energy introduced by their distinct polarity. This and the bonding regularities often lead to further specific ordering of the atoms in special structure types (coloring effects), not only in the many types enumerated above but also in some shell-type (multiply endohedral) structures as found, for example, for certain quasicrystal approximant systems.[17]

One important structural characteristic in this area that has caught our attention is the dominance of often complex, 3D networks among the less-explored alkaline-earth metal−triel phases, in binary and ternary systems that contain a d element. These nets characteristically encapsulate the cations in a 3D array to give each a high coordination number, the details of which are largely dependent on the relative sizes of the atoms, among other factors. These features often contrast with alkali-metal system structures (excluding Li) in which these lower-field cations are more often positioned on the outside of either anion arrays or more discrete or extended cluster anions, depending on the relative cation proportions. The latter persist with heteroatom substitutions in the network as well, that is, in $K_{34}In_{92.30}Li_{12.70}$, $K_3(Mg_{20}In_{14})$ and $K_{34}In_{91.05}Mg_{13.95}$.[18−20] The contrasting drive for high coordination numbers about the alkaline-earth elements with their higher (formal) charges leads to a more or less regular type of polyhedral construction in all the examples we have examined: *n*-vertex prisms centered by Ae that are further condensed into network polyanions in a manner that augments the Ae coordination about the waist of the original prisms.[9,11−12,21] This often means that prismatic atoms in adjoining units serve as waist atoms in the central one and vice versa. The same theme is found here.

Size matching for stabilization of these phases can be realized not only by means of cation alterations but also via substitution of other elements into the nominal polyanionic network. In our last report,[13] we demonstrated that substitution of the effectively smaller Au or Hg atoms into the sublattice of a $BaTl_2$ phase dramatically changes the structure from that of a hexagonal $CaIn_2$ type ($P6_3/mmc$) into the smaller orthorhombic $CeCu_2$ type (*Imma*), in which the fixed cation is better accommodated in a smaller distorted network. Herein we report two more examples in which the polar intermetallics $BaAu_2In_2$ (**1**) and $SrAu_2In_2$ (**2**) are generated in a new structure type (*Pnma*) from the respective $BaIn_4$ ($BaAl_4$-type,[22] I4/*mmm*) and $SrIn_4$ (self,[9] *C*2/m) by substitution of the effectively smaller Au for half of the In sites in the parent structures. The reduced symmetry for $SrIn_4$ is itself a good example of the effect that either an undersized cation or an oversized network has on a hypothetical $BaAl_4$-type parent.

Experimental Section

Syntheses. The high purity reagents were dendritic Ba and Sr (99.9%, Alfa-Aesar), Au sheet (99.997%, Ames Lab), and In teardrops (99.99%, Alfa-Aesar). These were handled in N_2-filled gloveboxes in which the moisture levels were controlled below 0.1 ppm (volume). The surface of the In was scraped clean with a scalpel before use, while the shiny samples of Ba and Sr were used as-is. The reactions were carried out in welded metal (Ta, Nb) tubing that was jacketed within evacuated fused silica containers and heated in resistance furnaces. The new structure does not form with Tl or Hg instead of Au in the presence of either In or Tl.[21]

In a search for new ternary Ba−Au−In intermetallics similar to hexagonal $BaAu_2Tl_2$,[21] single crystals of $BaAu_2In_2$ (**1**) were first obtained in about 70% yield, along with unknown phases, from a reaction with Ba/Au/In = 1:2:2, run at 1050 °C in welded Nb tubing, then quenched in water, and subsequently annealed at 1000 °C. A substantially pure single-phase **1** (>95%, no impurity lines detected) was subsequently obtained after the sample was annealed at 850 °C in Ta tubing for 16 h, as judged by comparison of the Guinier powder pattern with that calculated for the refined structure. (This result is illustrated in Supporting Information, Figure S1a.) Single crystals of $SrAu_2In_2$ (**2**) were also obtained in >95% yield from that ratio of elements in a welded tantalum tube that was heated at 1000 °C, quenched in water, annealed at 850 °C for 6 h, and subsequently, cooled at 5 °C h^{-1} to room temperature (Supporting Information, Figure S1b). Compositions with Au/In ratios of >1.35 or <0.75 in both systems contained other phases (Figures S3 and S4). Crystals of both compounds are silvery, brittle, and according to powder patterns, insensitive to moist air for up to 2 weeks as a powder and to liquid water over more than 10 min at room temperature (Figure S5). No surface changes visible with a light microscope were observed either.

Powder X-ray Diffraction. X-ray powder patterns of samples mounted between Mylar sheets were collected with the aid of a Huber 670 Guinier powder camera equipped with an area sensitive detector and Cu Kα radiation (λ = 1.540598 Å). The step size was set at 0.005°, and the exposure time was 30 min. Unit cell parameter refinements were obtained via the UNITCELL program.[23]

Structure Determinations. Silvery blocklike single crystals of **1** and **2** were mounted in thin-walled glass capillaries inside the glovebox and then transferred to Bruker Smart APEX CCD diffractometer for data collection at 293(2) K with Mo Kα radiation (λ = 0.71073 Å). A total of 1315 frames with an exposure time of 10 s each were collected for each. Intensities were integrated with the SAINT subprogram in the SMART software package[24] for the orthorhombic cell initially indicated from the indexing of 831 unique reflections from **1** and 817 reflections from **2**. Of these, 628 reflections for **1** and 567 reflections for **2** were observed [$I > 2\sigma(I)$]. The space group determination by the XPREP program in the SHELXTL 6.1 software package[25] indicated $Pna2_1$ (No. 33, CFOM = 4.92 for **1** and 4.60 for **2**) or *Pnma* (No. 62, CFOM = 2.57 for **1** and 2.71 for **2**), but the intensity statistics did not show very clear indications of centricity ($|E^2 - 1| = 0.903$ for **1** and 0.893 for **2**). However, refinements for both proceeded successfully in centrosymmetric *Pnma*. Empirical absorption corrections were made

(15) Galadzhun, Y. V.; Hoffmann, D.-R.; Poettgen, R.; Adam, M. *J. Solid State Chem.* **1999**, *148*, 425.
(16) Li, B.; Corbett, J. D. *J. Am. Chem. Soc.* **2006**, *128*, 12392.
(17) Lin, Q.; Corbett, J. D. *Proc. Natl. Acad. Sci. U.S.A.* **2006**, *103*, 13589.
(18) Li, B.; Corbett, J. D. *J. Am. Chem. Soc.* **2005**, *10*, 926.
(19) Li, B.; Corbett, J. D. *Inorg. Chem.*, **2006**, *45*, 3861.
(20) Li, B.; Corbett, J. D. *Inorg. Chem.* **2006**, *45*, 8958.
(21) Dai, J.-C.; Palasyuk, A.; Corbett, J. D. Unpublished research.
(22) Bruzzone, G. *Acta Crystallogr.* **1965**, *18*, 1081.
(23) Holland, T. J. B.; Redfern, S. A. T. *Mineral. Mag.* **1997**, *61*, 65−77.
(24) *SMART*; Bruker AXS, Inc.; Madison, WI, 1996.
(25) *SHELXTL*; Bruker AXS, Inc.; Madison, WI, 2000.

Table 1. Some Crystal and Structural Refinement Parameters for 1 and 2

	1	2
empirical formula	$BaAu_2In_2$	$SrAu_2In_2$
fw	760.91	711.19
space group, Z	*Pnma* (No. 62), 4	*Pnma* (No. 62), 4
unit cell dimensions[a]		
a (Å)	8.755(2)	8.530(2)
b (Å)	4.712(1)	4.598(1)
c (Å)	12.368(3)	12.283(4)
V (Å^3)	510.1(2)	481.7(2)
d_{calcd} (Mg m^{-3})	9.906	9.801
μ (Mo Kα) (mm^{-1})	73.62	80.88
final indices[b]		
R1	0.0442	0.0387
wR2 [$I > 2\alpha(I)$]	0.1157	0.0942

[a] Refined from Guinier powder data. [b] $R1 = \sum(||F_o| - |F_c||)/\sum|F_o|$; $wR2 = \{\sum w[(F_o^2 - F_c^2)^2]/\sum w[(F_o^2)^2]\}^{1/2}$.

Table 2. Atomic Positions ($\times 10^4$) and Isotropic Displacement Parameters ($\times 10^3$ Å^2) for **1** and **2**

atom	Wyckoff	x	y	z	U(eq)
		1 $BaAu_2In_2$			
Au1	4*c*	894(1)	2500	209.8(7)	12(1)
Au2	4*c*	261(1)	2500	6638.2(7)	17(1)
In1	4*c*	3969(2)	2500	492(1)	12(1)
In2	4*c*	3597(2)	2500	6412(1)	12(1)
Ba	4*c*	2801(1)	2500	3339(1)	12(1)
		2 $SrAu_2In_2$			
Au1	4*c*	931(1)	2500	157(1)	11(1)
Au2	4*c*	93(1)	2500	6695(1)	13(1)
In1	4*c*	4040(2)	2500	520(1)	11(1)
In2	4*c*	3469(2)	2500	6394(1)	10(1)
Sr	4*c*	2894(2)	2500	3325(2)	12(1)

with SADABS program[26] for **1** and with ψ-scans for **2**. Finally, both structures were solved by direct methods with the aid of SHELXTL 6.1 and refined by full-matrix least-squares on F_o^2, ultimately with anisotropic thermal parameters and a secondary extinction parameter. These converged at R1 = 4.42% for **1** and 3.87% for **2**. All positions were fully occupied by single atom types. The largest residual peak and hole in the ΔF map for **1** were 3.63 and −4.79 e Å^{-3}, and for **2**, 5.64 and −2.74 e Å^{-3}: all <1.40 Å from network atoms. Some crystallographic data for each are summarized in Table 1, and the atom positions and important bond lengths are listed in Tables 2 and 3, respectively. More detailed crystallographic and refinement information, as well as anisotropic displacement parameters, are available in Supporting Information.

Property Measurements. Electrical resistivities of **1** were determined on 113.3 mg of sample with grain diameters between 150 and 250 μm that was dispersed within chromatographic alumina inside the glovebox and then sealed in a Pyrex tube. Measurements were made at 34 MHz over the range of 80−280 K by the electrodeless "Q" method with the aid of Hewlett-Packard 4342A Q meter.[27] Magnetic susceptibility measurements were carried out between 1.8 and 350 K with the aid of a Quantum Design (MPMS) SQUID magnetometer. Polycrystalline samples, 131.9 mg of **1** and 107.5 mg of **2**, were held between faces of two fused silica rods as described previously.[28]

Calculations. Electronic band structure calculations were made by the extended Hückel tight-binding (EHTB) method with the aid of the CAESAR software developed by Whangbo and co-workers.[29] The parameters (valence energies (eV), orbital exponents) used were as follows: Ba, 6s −5.21, 1.21; 6p −3.43, 1.21, 5d −3.99, 4.33, 0.688, 1.64 0.595; Sr, 5s −5.69, 1.214; 5p −3.87, 1.214, 4d −3.37, 3.047,0.7492, 0.9885, 0.5467;[30] In, 5s −12.6, 1.903; 5p −6.19, 1.677;[31] Au, 6s −10.92, 2.602; 6p −5.55, 2.584; 5d −15.076, 6.163, 0.6851, 2.794, 0.5696.[32]

Table 3. Important Bond Lengths (Å) in **1** and **2** and the Corresponding Mulliken Overlap Population Values (MOP)

bond	bond length	MOP	bond	bond length	MOP
			1 $BaAu_2In_2$		
Au1−In1	2.715(2)	0.45	Au2−In2	2.818(2)	0.52
Au1−In2 (×2)	2.821(1)	0.36	Au2−In1 (×2)	2.831(1)	0.38
Au1−In2	2.840(2)	0.36	Au2−In1	2.867(2)	0.31
Au1−Au1 (×2)	2.876(1)	0.16	Au2−In2	2.934(2)	0.32
Au1−Ba	3.249(2)	0.01	Au2−Ba (×2)	3.569(1)	0.02
Au1−Ba (×2)	3.494(1)	0.01	Au2−Ba (×2)	3.585(1)	0.02
In1−Au1	2.715(2)	0.45	In2−Au1 (×2)	2.821(1)	0.36
In1−Au2 (×2)	2.831(1)	0.38	In2−Au1	2.840(2)	0.36
In1−Au2	2.867(2)	0.31	In2−Au2	2.818(2)	0.52
In1−In1 (×2)	3.208(2)	0.28	In2−Au2	2.934(2)	0.32
In1−In2 (×2)	3.448(1)	0.17	In2−In1 (×2)	3.448(1)	0.17
In1−Ba	3.653(2)	0.04	In2−Ba (×2)	3.568(2)	0.07
In1−Ba	3.667(2)		In2−Ba	3.863(2)	
In1−Ba (×2)	3.879(2)		In2−Ba (×2)	3.949(2)	
Ba−Au1	3.249(2)	0.01	Ba−In1	3.667(2)	0.02
Ba−Au1 (×2)	3.494(1)	0.01	Ba−In1 (×2)	3.879(2)	
Ba−Au2 (×2)	3.569(1)	0.02	Ba−In2 (×2)	3.568(2)	0.07
Ba−Au2 (×2)	3.585(1)	0.02	Ba−In2 (×2)	3.949(2)	
Ba−In1	3.653(2)	0.04	Ba−In2	3.863(2)	
			2 $SrAu_2In_2$		
Au1−In1	2.690(2)	0.44	Au2−In2	2.726(2)	0.56
Au1−In2 (×2)	2.8034(9)	0.34	Au2−In1 (×2)	2.8139(9)	0.35
Au1−In2	2.836(2)	0.33	Au2−In1	2.865(2)	0.28
Au1−Au1 (×2)	2.8219(8)	0.18	Au2−In2	2.904(2)	0.30
Au1−Sr	3.193(2)	0.04	Au2−Sr (×2)	3.433(2)	0.05
Au1−Sr (×2)	3.371(2)	0.04	Au2−Sr (×2)	3.500(2)	0.041
In1−Au1	2.690(2)	0.44	In2−Au1 (×2)	2.8034(9)	0.34
In1−Au2 (×2)	2.8139(9)	0.35	In2−Au1	2.836(2)	0.33
In1−Au2	2.865(2)	0.28	In2−Au2	2.726(2)	0.56
In1−In1 (×2)	3.099(2)	0.30	In2−Au2	2.904(2)	0.30
In1−In2 (×2)	3.320(2)	0.19	In2−In1 (×2)	3.320(2)	0.19
In1−Sr (×2)	3.581(2)	0.05	In2−Sr (×2)	3.502(2)	0.08
In1−Sr (×2)	3.909(2)		In2−Sr	3.802(2)	0
			In2−Sr (×2)	3.878(2)	
Sr−Au1	3.193(2)	0.04	Sr−In1 (×2)	3.581(2)	0.05
Sr−Au1 (×2)	3.371(2)	0.04	Sr−In2 (×2)	3.502(2)	0.08
Sr−Au2 (×2)	3.433(2)	0.05	Sr−In2	3.802(2)	0
Sr−Au2 (×2)	3.500(2)	0.04	Sr−In2 (×2)	3.878(2)	
Sr−In1 (×2)	3.909(2)				

Results and Discussion

Structure. The isostructural $BaAu_2In_2$ (**1**) and $SrAu_2In_2$ (**2**) can be synthesized directly in high yields. They crystallize in a new ordered structural type (*Pnma*), which differs significantly from (a) a family of related tetragonal $BaAl_4$-type structures (I4/*mmm*) known for $BaIn_4$,[22] $BaAuIn_3$,[12] $SrAuIn_3$ (unpublished, Supporting Information), $BaPt_xIn_{4-x}$ ($x = 0-1$), and $BaHg_xIn_{4-x}$ ($x = 0-2$)[21] and (b) monoclinic $SrIn_4$ (*C*2/m, No. 12).[9,33] The new structure, Figure 1, consists of a rather complex $_\infty{}^3[Au_2In_2]^{2-}$ polyanionic network that

(26) Blessing, R. H. *Acta Crystallogr.* **1995**, *A51*, 33.
(27) Zhao, J.-T.; Corbett, J. D. *Inorg. Chem.* **1995**, *34*, 378.
(28) Guloy, A. M.; Corbett, J. D. *Inorg. Chem.* **1996**, *35*, 4669.
(29) Ren, J.; Liang, W.; Whangbo, M.-H. *CAESAR for Windows*; Prime-Color Software, Inc., North Carolina State University: Raleigh, NC, 1998.
(30) (a) Brennan, T. D.; Burdett, J. K. *Inorg. Chem.* **1993**, *32*, 746. (b). Seo, D.-K.; Corbett, J. D. *J. Am. Chem. Soc.* **2002**, *124*, 45.
(31) Hinze, J.; Jaffé, H. H. *J. Chem. Phys.* **1963**, *67*, 1501.
(32) Komiya, S.; Albright, T. A.; Hoffmann, R.; Kochi, J. K. *J. Am. Chem. Soc.* **1977**, *99*, 8840.
(33) Fornasini, M. L.; Ciafici, S. *Z. Kristallogr.* **1990**, *190*, 295.

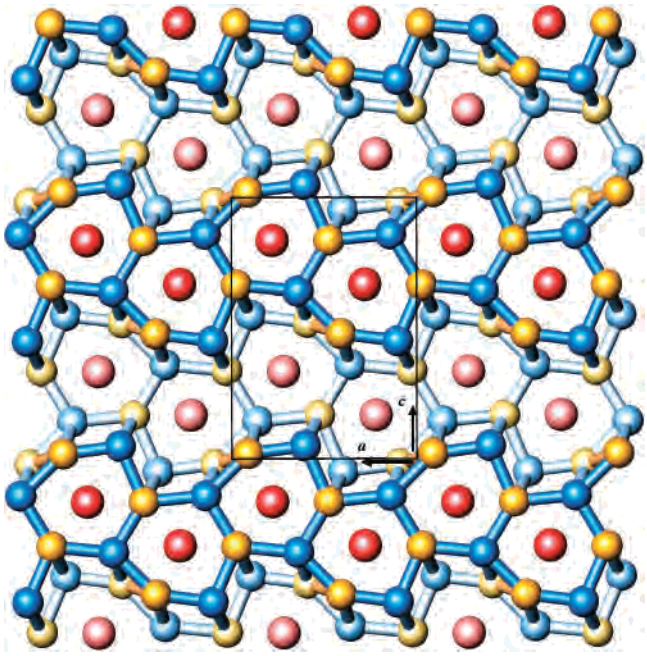

Figure 1. [010] Projection of the orthorhombic (*Pnma*) structure of AeAu$_2$-In$_2$ (Ae = Ba, Sr) with Ae as red, Au as gold, and In as blue spheres. These define, in projection, Ae-centered hexagonal prisms of alternating Au and In atoms that share rectangular (side) faces to generate infinite zigzag chains of prisms along *a*. The lighter colored chains of the same construction are displaced into the Figure by *b*/2 such that those nearer prismatic atoms are coplanar with the adjoining Ae and augment the bonding to it.

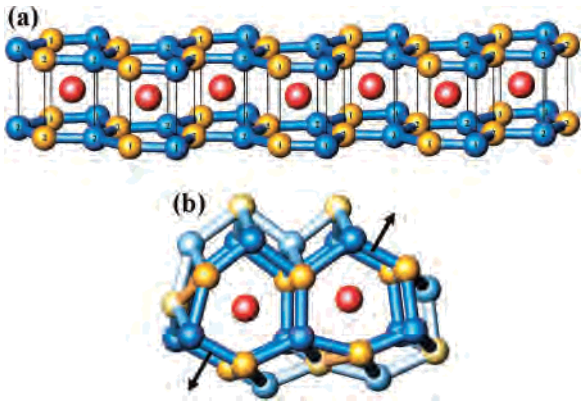

Figure 2. (a) Single zigzag chain of hexagonal prisms in AeAu$_2$In$_2$ that share pairs of edges. (b) The pair of prisms viewed along *b* that constitutes the independent unit in AeAu$_2$In$_2$. The arrows mark the faces on which the condensation continues.

encapsulates Ba (or Sr) cations within augmented hexagonal prisms constructed of In and Au. (The Sr member is appropriately smaller but otherwise not distinctive, and it will not be considered further.) The structure is important in the generality of its nature, and therefore, a description of this in steps follows. The prisms are constructed from parallel hexagons (eclipsed in this view), each of alternating Au and In atoms, namely, Au1, Au2 (×2), In1, and In2 (×2), that are separated by ∼4.7 Å (*b* axis) and centered by Ba. All atoms lie on mirror planes at $y = 1/4$ and 3/4. The hexagonal prisms further share pairs of rectangular (side) faces to generate the next building block, zigzag chains of prisms that run along $\vec{a}$, as shown in Figure 2a in isolation and in Figure 1 in the whole structure (Ba, red; In, blue; Au, gold). (These chains also share opposed hexagon faces along $\vec{b}$ to generate infinite puckered sheets, but this simple feature is not very important to understanding the overall result.) The zigzag chains, alternately displaced by *b*/2, are further condensed side by side along $\vec{c}$, Figure 1, resulting in each Ba gaining additional coplanar Au and In neighbors around the waists of the hexagonal prisms. The otherwise equivalent darker- and lighter-colored chains in Figure 1 are designed only to make this condensation aspect clearer. (In detail, this motif follows from the *n* glide; a reflection in *a* followed by combined translations of *c*/2 and *b*/2.)

As can been seen, zigzag chains of rhomboids constitute the seams between adjoining chains of hexagonal prisms, these naturally being splayed outward (i.e., the chains are somewhat further apart); because these lighter-colored augmenting atoms lie in the plane of the barium atoms. The net result of this displacement and the essence of the local polyhedral array about Ba are illustrated in the simple repeat unit shown in Figure 2b. Here two hexagonal prisms share a face (In2,Au2)$_2$ and are further decorated by two strings of five lighter-colored In, Au atoms (1,2,2,1,1) that lie in the plane of the Ba atom. Note that these strings have opposite atom identities around an imagined 2-fold axis in the shared face and that these atoms are also located nearer the outside *edges* of the hexagonal prisms, not outside the faces. The last is probably a reflection of the fact that two (In2,Au2)$_2$ faces on each prism are excluded because they are shared with further hexagonal prisms (arrows) to generate the zigzag chains. Otherwise, the roles of the outer atom are much the same as those of the capping atoms in the much more familiar environments about condensed tricapped trigonal prisms, and likewise, both types have similar dual functions.

The driving force for packing these five additional polyanion atoms around Ba certainly must originate with the polarity differences, which appear to drive the system toward a maximum coordination number around the relatively large Ba (or Sr) atoms. This appears to be a generality in several structures of related compounds (below). Still, the polyhedron of 12 + (4 − 6) neighbors about each Ae is not very regular, doubtlessly because of packing and condensation limitations. The Ba−In and Ba−Au distances within the hexagonal prisms show, respectively, a modest 3.57−3.95 Å and a narrower 3.49−3.58 Å range. The former are comparable to the additional distances from Ba to coplanar waist atoms, 3.65 and 3.67 Å to In1 and 3.86 Å to In2, but the short 3.25 Å distance for Ba−Au1 is especially notable. The practical coordination number of Ba is best described as 16. The waist Au1 and Au2 atoms at the top of Figure 2b are not well bonded to Ba here (d > 4.2 Å), but they are well bonded to the cation in the adjoining lighter-colored hexagonal prisms displaced into the projection by *b*/2, Figure 1. In general, the augmenting atoms about the waist in one prismatic unit in these kinds of motifs are members of hexagonal prisms in the neighboring chains and vice versa.

Note that nearly all good bonding contacts in this network are heteroatomic Au−In, 2.69−2.93 Å, except for a pair of somewhat long Au−Au contacts at 2.87 (2.82) Å near the shared face. (The Pauling metallic single bond length is 2.68

Å.)[34] This contact may result from more of a matrix (packing) effect. (It is the short diagonal of a rhomboid with ~120° angles at Au and ~60° at In.). The shortest Au1−In1 distances here, 2.72 and 2.69 Å with Ba and Sr, respectively, are roughly comparable to those in $BaAl_4$-type $AeAuIn_3$, 2.77[12] and 2.70 Å (SI), respectively, in which these occur between equivalent 50−50-mixed In/Au positions. (Some matrix effect from Ba may be reflected by the larger value in $BaAuIn_3$.) The shortest Au−In distances here are also 0.10 and 0.16 Å less than those in the corresponding $AeAuIn_3$. In contrast, all In−In separations in the title phases are (≥3.21 Å = In1(prism)−In1(waist)) relatively long[16,18,19] and not marked in the figures. The In atoms have six network neighbors up to this limit, and the Au atoms have five or six, the latter also having one fewer Ae neighbor, perhaps because of their somewhat smaller effective sizes. The presumed greater strength of heteroatomic (versus homoatomic) bonding in this type of structure may be responsible for the formation of numerous compounds of this nature between the triels and gold or its neighbors.[21] A second polarity (or bond strength) factor influencing the stability of this and many related Ae−Au−Tr structures and compositions can also be imagined according to the extremes in Mulliken electronegativity values for these three atom types: Ae, 2.0−2.4; In, 3.1; Au, 5.77 eV.[35]

General Motif. The evident tendency to maximize the coordination numbers of Ae cations in many compounds of this sort also means that there are close size correlations between the cation sizes and their evidently tight fit within the polyanionic networks. In addition, two or more kinds of network atoms appear to afford greater flexibility in the polyhedral construction and their ordered arrangements. Thus, independent adjustments of either the cations or of some atoms in the anionic network will result in bond length alterations, and these may drive a structural change. A change in stoichiometric proportions naturally leads to a structural change as well, but the general motif of a tight fit between the cation and network atom sizes still persists and often with similarly augmented prismatic units. Recently described results span a variety of augmented ring systems of different sizes and interconnections. Figure 3 a−d shows analogous projections of four other distinctive network arrays in phases that also have overall 1:4 stoichiometries and involve at least one pair of augmented prisms sharing rectangular edges. These are (a) the higher-symmetry prototype $BaIn_4$[22] ($BaAl_4$-type), (b) the unusual $BaHg_2Tl_2$[21] (in which ordering if any could not be ascertained by X-ray diffraction), (c) the distorted consequence of too small of a cation in a, monoclinic $SrIn_4$[9] (self) (and also $BaTl_4$[21]), and (d) another mixed Au/Tl example in Ba_2AuTl_7,[11] all of which compare with the equivalent structural unit in $AeAu_2In_2$, Figure 2b.

The higher-symmetry $BaIn_4$ member, Figure 3a, is ideally proportioned so that the unit shown basically shares all four 6-rings about the waist of the cell in a common tetragonal structure type. This gives the cation eight close In neighbors

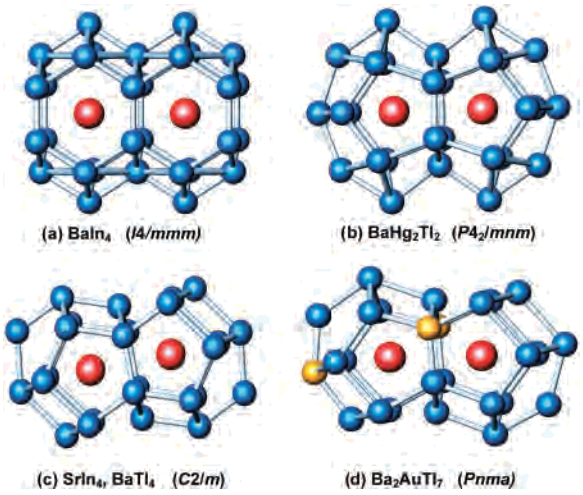

Figure 3. Four examples of pairs of augmented prisms of In,Tl/Au,Hg polyanions that enclose Ba or Sr atoms: (a) the tetragonal $BaAl_4$-type example for $BaIn_4$, (b) the basic unit in tetragonal $BaHg_2Tl_2$, (c) the unit in monoclinic $SrIn_4$ and $BaTl_4$, and (d) the independent unit in orthorhombic Ba_2AuTl_7. Examples c and d differ further in additional condensation details.

in the four cell faces plus eight somewhat more distant In contacts in the square planer layers normal to $\vec{c}$ (meaning that the 6-rings are somewhat elongated). The structure has been well considered in terms of its significant restrictions in the relative sizes of the cation and the network (among other things).[36−38] The other three uniaxial members (b−d) contain only pairs of face-sharing Ae-centered pentagonal prisms rather than the infinite chains of these in the present analogues. All are infinitely condensed along the view direction, but they differ appreciably in augmentations about the waists of the prisms which arise via different complex ways in which adjoining prismatic columns displaced by one-half of the projection length are condensed. The novel $BaHg_2Tl_2$ structure, 3b, has a higher symmetry than the others and augmentation by 7-rings as well (a 4_2 axis runs through the shared face), but these units do not show further side face condensation. The $SrIn_4$ structure in 3c (and, unparallel, $BaTl_4$) can be viewed as the result of cation−network size mismatching, the Sr (Ba) atoms in $BaIn_4$ ($BaTl_4$) being too small to support the $BaAl_4$-type tetragonal In(Tl) network. But the shortening of some bonds in the latter through random substitution of 50% Au in the closer waist positions (because of relativistic effects)[39] restores the tetragonal structure (3a) in a smaller $SrAuIn_3$.[12] (Substitution of Zn or Mg in other reactions also shrink the cage and produce the same parent structure type.)[40] Finally, the ordered substitution of 12% Au into the $BaTl_4$ network, 3c, gives the novel Ba_2AuTl_7 result in Figure 3d. Although the local geometries of the last two models look very similar (except for the Au substitution), other changes are also present in the bigger picture, still of the character of how inner prismatic atoms

(34) Pauling, L. *Nature of the Chemical Bond*, 3rd ed.; Cornell University Press: Ithaca, NY, 1960; p 403.
(35) Pearson, R. G. *Inorg. Chem.* **1988**, *27*, 735.
(36) Zheng, C.; Hoffmann, R. *Z. Naturforschung.* **1986**, *41B*, 292.
(37) Burdett, J.; Miller, G. J. *Chem. Mater.* **1990**, *2*, 12.
(38) Häussermann, U.; Amerioun, S.; Eriksson, L.; Lee, C.-S.; Miller, G. J. *J. Am. Chem. Soc.* **2002**, *124*, 4371.
(39) (a) Pyykkö, P. *Chem. Rev.* **1988**, *88*, 63. (b) Pyykkö, P. *Angew. Chem., Int. Ed.* **2002**, *41*, 3573.
(40) Li, B.; Corbett, J. D. Unpublished research.

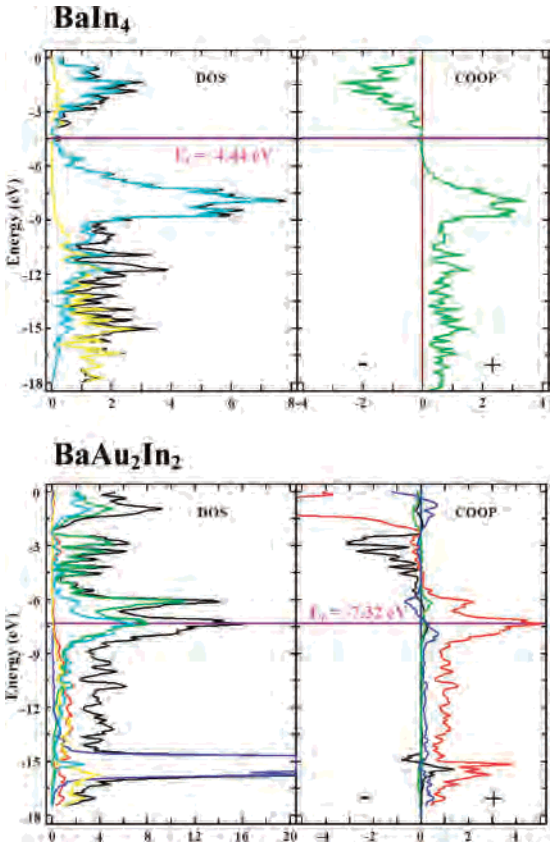

Figure 4. Extended Hückel calculation results for $BaIn_4$ (top) and $Ba_2Au_2In_2$ (bottom). The black lines in the DOS results mark the totals. The red, green, and blue indicate Au s, Au p, and Au d, and the yellow and cyan indicate In s and In p in the PDOS, respectively. The COOP data are green for In−In, red for Au−In, and black for Au−Au bonding.

in one cage are also augment atoms in adjoining units displaced by *b*/2 but somewhat more complex in detail. It should also be noted that the presence of 6-rings, rather than 5-rings, in the title phases, Figure 2b, in contrast to the 5-ring examples in Figure 3b−d (and elsewhere), doubtlessly results from 0.10 to 0.16 Å shorter In−Au distances relative to the In−In ring bonds and the size of Ba.

Some further generalities regarding such augmented prismatic constructions can be seen in the literature for other similar elements and stoichiometries, that is, $SrAu_3In_3$ (*Pmmn*), $Sr_4Au_9In_{13}$ (*P*-6), $SrIn_{5-x}Tl_x$ (*Pmmn*, $x \approx 1.4$), $BaPt_xIn_{4-x}$ (*P*4/*nmm*, $x \approx 1.4$),[21] and $Ca_2Au_3In_4$ (*Pnma*).[14] Condensed zigzag chains in the last are similar to those reported here, except that packing considerations mean that the linear portions are three prisms long rather than two. The stoichiometries $CaTnIn_4$ exist in two different and less-related structures depending on whether Tn is in the Co or the Ni family.[21,41] A more complex arrangement has been found in $(Sr,Eu)_2Au_3In_4$ and $Sr_2Pt_3In_4$ (*P*-62*m*, $Hf_2Co_4P_3$-type). Here, groups of three augmented hexagonal prisms that share a common edge are separated by 5- and 6-fold prisms that appear to share some inner prismatic atoms with the former groups.[14] Not surprisingly, the relatively simple principles noted here do not apply as well in some analogues containing trivalent lanthanides.[15,42]

(41) Hoffmann, D.-R.; Poettgen, R. *Chem.—Eur. J.* **2000**, *6*, 600.

Electronic Structure and Chemical Bonding. Figure 4 shows the total and projected partial densities of states (DOS) and the crystal orbital overlap populations (COOP) computed by EHTB methods for $BaIn_4$ (with positional parameters from Bruzzone),[35] as well as for $BaAu_2In_2$. Starting with $BaIn_4$ (top, tetragonal), the DOS values suggest that the phase is probably weakly metallic, and the COOP result suggests that the In−In bonding is optimized. Substitution of one-half of the In by Au to give the orthorhombic $BaAu_2In_2$ (bottom figure) backs the Fermi energy down onto the valence bands, which are principally Au p and In p at this point, and introduces a low-lying Au $5d^{10}$ band. The dominant Au−In bonding (red curve) is now far from optimized in the sense that empty bonding states remain, while the minor In−In and Au−Au bonding components (green and black) are close to optimal. Calculations on the intermediate tetragonal $BaAuIn_3$[12] (Figure S10, Supporting Information) yield substantially intermediate results both in the location of E_F on the valence band and in the lack of optimization of particularly the In−M bonding (M = 50:50 Au/In) and, to a lesser degree, M−M. These relatively simple calculations still probably underestimate the contributions of the Au s and Ae d states to the bonding judging from the results of better ab initio calculations on similar compounds.[16,43]

We have to this point ignored the fact the pronounced shortening of the In−Au bonds achieved in the title phases relative to those in the all-indium analogues might originate with the removal of antibonding electrons, as improbable as this might seem for such electron-poor compounds. But the above band results indicate that the states being emptied on substitution of gold for indium are instead bonding. This result seems to be general for this type of substitution chemistry, although this feature needs to be explored.

Physical Properties. The measured specific resistivity of **1** is ~41 $\mu\Omega$ cm at room temperature with a mean temperature dependent on 4.3% K^{-1}, indicating a metallic behavior as predicted (Figure S6, Supporting Information). The temperature dependencies of the magnetic susceptibilities of **1** and **2** measured at 3 and 1 T upon heating are also shown in Supporting Information (Figures S7 and S8). The susceptibilities of **1** are rather small, positive, and almost temperature independent with values of $\chi_m \approx 9.4 \times 10^{-4}$ emu mol^{-1} at 3 T and $\chi_m \approx 2.3 \times 10^{-3}$ emu mol^{-1} at 1 T over the range of 5−350K, suggesting that the compound is essentially Pauli paramagnetic, consistent with the expected metallic character. The magnetic susceptibilities of **2** are similar with $\chi_m \approx 5.9 \times 10^{-5}$ emu mol^{-1} at 3 T and $\chi_m \approx 6.3 \times 10^{-3}$ emu mol^{-1} at 1 T over the range of 25−350 K, typical of a Pauli paramagnetic characteristic.

Acknowledgment. We are indebted to S. Budko for the magnetic susceptibility data. This research was supported by the Office of the Basic Energy Sciences, Materials

(42) Galadshun, Y. V.; Zaremba, V. I.; Kalyshak, Y. M.; Hoffmann, D.-R.; Poettgen, R. *Z. Anorg. Allg. Chem.* **2000**, *626*, 1773.
(43) Li, B.; Corbett, J. D. *Inorg. Chem.* **2007**, *46*, 2237.

Sciences Division, U.S. Department of Energy (DOE). The Ames Laboratory is operated for DOE by Iowa State University under Contract No. DE-AC02-07Ch11358.

Supporting Information Available: Additional crystallographic information for **1**, **2**, and $SrAuIn_3$, powder pattern data for both the formation of the two $AeAu_2In_2$ in the pseudobinary systems and the stability of **1** to air/moisture, and resistivity and magnetic susceptibility data for **1** and **2**. This material is available free of charge via the Internet at http://pubs.acs.org.

IC070142V